Ye et al | Article 11040
J Pure Appl Microbiol. 2026;20(2):1414-1428. doi: 10.22207/JPAM.20.2.28
Received: 11 October 2025 | Accepted: 18 February 2026
Published Online: 18 May 2026

P-ISSN: 0973-7510; E-ISSN: 2581-690X

RESEARCH ARTICLE OPEN ACCESS

Isolation and Biological Characterization of a *Yersinia pestis* Bacteriophage HQG8 from Domestic Dogs in a Chinese Plague Focus

Lingling Ye[1], Binghang Lyu[2], Shengdan Li[3] and Xiaoling Zhu[1]*

[1]The First Affiliated Hospital, Dali University, Dali City, Yunnan Province, China.
[2]International Exchange and Cooperation Division, Dali University, Dali City, Yunnan Province, China.
[3]Faculty of Nursing, Dali University, Dali City, Yunnan Province, China.

Abstract

To investigate the presence of plague phages in dogs, we isolated one plague phage strain from 15 anal swab samples from Chinese field spaniels, an indicator animal species in the source area of newly emerging wild rat plague in Yunnan Province, China, in April 2024. Isolation and purification of the phage strain were performed using the double-layer agar plate method. Titer was determined using the spot plate and drop methods, and a one-step growth curve was plotted using the classical method. Observations through transmission electron microscopy showed that the isolated plague phage (HQG8) has a typical tadpole morphology, consisting of an icosahedral head, an intermediate annular neck ring, and a long contractible tail sheath. HQG8 showed lysis of multiple *Yersinia pestis* strains at 28 °C and 37 °C, and it exhibited lytic activity against *Shigella flexneri* 2a at 22, 28, and 37 °C. The optimal multiplicity of infection-ratio of phage particles to host bacteria at the time of infection for HQG8 was 0.1. The incubation and lysis periods were approximately 40 min and 140 min, respectively, and growth entered the stabilization period after 180 min. Genomic analysis showed that the total length of the gene sequence of HQG8 is 35,876 bp. To our knowledge, this is the first study to isolate the *Y. pestis* bacteriophage from domestic dogs during a wild rodent plague in China. Although genomic analysis revealed that HQG8 is highly similar to previously reported phages infecting *Enterobacteriaceae*, its isolation from a canine host within a plague ecosystem is unprecedented. Our findings provide new insights into the ecology of plague phages and highlights dogs as potential reservoirs for bacteriophages that may influence the dynamics of *Y. pestis* in natural foci.

Keywords: *Yersinia pestis*, Bacteriophage, Plague Focus, Isolation, Biological Characterization

***Correspondence:** 2008zhuzhuxiaoling@163.com

Citation: Ye L, Lyu B, Li S, Zhu X. Isolation and Biological Characterization of a *Yersinia pestis* Bacteriophage HQG8 from Domestic Dogs in a Chinese Plague Focus. *J Pure Appl Microbiol.* 2026;20(2):1414-1428. doi: 10.22207/JPAM.20.2.28

INTRODUCTION

Bacteriophages are the most abundant organisms in the biosphere and are ubiquitous features of prokaryotic existence.[1] They are viruses that invade bacteria, disrupting their metabolism, leading to lysis (lytic phages).[2] Plague phages specifically infect *Yersinia pestis*. They can be classified into various types, including filamentous bacteriophages, such as YpfΦ, and lytic bacteriophages, such as JC221, MHS112, and GMS130.[3] These bacteriophages have diverse morphologies and biological characteristics and are widely present in the animals of natural plague foci.[4] Plague bacteriophages have various structural differences; for example, JC221, which belongs to the family Myoviridae has a regular icosahedral head and long tail. Its genome is double-stranded DNA containing hundreds of genes.[5] Some bacteriophages, such as YpfΦ can integrate into the chromosomes of *Y. pestis* to become stable probacteriophages and affect the virulence and evolution of the strain.[6]

Phages have been effectively used to treat various bacterial diseases.[7] Plague bacteriophages can be used for rapid and specific detection of *Y. pestis*,[8] and some engineered bacteriophages emit bioluminescent signals within a few minutes after infection, facilitating rapid diagnosis of clinical and environmental samples.[9] In addition, phage therapy has shown potential against multidrug-resistant *Y. pestis* in animal models; its use alone or in combination with antibiotics can significantly improve survival rates.[10] The diversity and wide distribution of plague bacteriophages help form an ecological barrier and inhibit the spread of *Y. pestis* in natural foci.

The conventional isolation of bacteriophages relies on environmental and biological sampling from plague reservoirs. The key sampling sites have included the Qinghai–Tibet Plateau, Mongolia, and other endemic zones characterized by active rodent populations. Samples have been obtained from soil, water bodies, and infected host animals. In recent years, metagenomic technology has been used to mine phage sequences directly from environmental samples, thereby accelerating the discovery of new phages. In most cases, attenuated strains of *Y. pestis* (such as EV76) or closely related species (such as *Yersinia pseudotuberculosis*) are used for enrichment culture. The double-layer agar plate method, which combines centrifugal filtration and chloroform treatment to remove bacterial debris, is the mainstream method. Most *Y. pestis* bacteriophages show a narrow host spectrum and only infect specific serotypes of *Y. pestis*, but some broad-spectrum bacteriophages can cross-species lyse *Y. pseudotuberculosis*.[11] Significant progress has been made in the research of plague bacteriophages regarding isolation techniques, functional genomics, and synthetic biology modification. However, their application still faces challenges in host specificity, drug resistance, and safety.

Most studies have focused on a few common hosts, such as marmots and yellow rats; however, systematic comparisons of whether specific bacteriophages are present in the intestines, blood, or body surfaces of different rodent or carnivore species are still lacking.[12] Although rodents are well-studied reservoirs, phage dynamics in carnivores such as dogs are poorly understood. Biological characterization can reveal the fundamental properties of *Y. pestis* bacteriophages, including their classification, morphological structure, and life cycle, and only after understanding the basic characteristics of these bacteriophages can we better study their interactions with *Y. pestis* and explore their microscopic molecular biological information.[13]

In this study, we hypothesized that dogs with plague foci harbor phages that modulate *Y. pestis* persistence. Plague bacteriophages were isolated from dogs in wild rat plague foci in Yunnan Province, China. Dogs serve as "indicator animals" in this endemic area. Although, to date, there are no cases of dogs in the Yunnan Province being infected with plague bacteria and falling ill or dying, whether the plague bacteriophages produced in the dogs' bodies after being infected with plague bacteria have a protective effect still requires in-depth exploration. These dogs are in close contact with humans; therefore, characterizing the bacteriophages they carry is epidemiologically relevant, as it may inform local plague surveillance and control strategies.

MATERIALS AND METHODS

Biosafety and biocontainment statement

All experimental procedures involving *Y. pestis* were conducted under strict Biosafety Level 2 (BSL-2) containment conditions in a certified laboratory at the Yunnan Provincial Institute for Endemic Disease Control. The authorization was based on the use of the attenuated, avirulent strain *Y. pestis* EV76, which is exempt from higher-level containment requirements as per the World Health Organization (WHO) Laboratory Biosafety Manual and relevant Chinese biosafety regulations. All personnel were trained in BSL-2 practices and procedures, including the use of personal protective equipment (PPE) such as lab coats, gloves, and safety glasses. Bacterial cultures and phage lysates were manipulated within a Class II biological safety cabinet. All liquid and solid waste containing biological materials were inactivated by autoclaving at 121 °C for 30 min prior to disposal.

Preparation of host bacteria

A pure EV76 master board was prepared and stored at 4 °C until use. Weak strains of *Y. pestis* EV76 were selected from the mother plate in the biosafety cabinet and placed on agar plates. The plates were densely streaked and then incubated in a constant temperature box at 28 °C for 18-24 hrs until the logarithmic growth phase of the bacteria. Individual colonies were selected from the agar plates using inoculation rings and placed in 8 mL of LB (Luria-Bertani) medium. The agar plates were then incubated at 180 rpm and 28 °C until the logarithmic growth phase.

Sample processing

Anal swab samples were collected from the dogs. First, the dogs were secured using a special dog clamp, then the perianal area of the dogs was disinfected from the inside with 0.18%-0.23% iodophor. A disposable, medically sterilized cotton swab was inserted 3-5 cm into the anus of the dog. The cotton swab was gently rotated clockwise and then placed in prepared modified PBS (Phosphate Buffered Saline) enrichment solution. The samples were labelled and stored at 4 °C until further analysis.

In the biosafety cabinet, 1 mL of the dog anal swab enrichment solution (cold-inoculated with PBS at 4 °C for 15-20 days) was added to a 1.5 mL centrifuge tube and centrifuged at 8,000 × *g* for 2 min and the supernatant was subsequently collected. The canine anal swab samples collected were grouped for batch processing. Ten samples were used to form groups. The supernatant was filtered through a 0.22 µm microporous membrane, the filtrate was collected in 50 mL centrifuge tubes, labelled as HQG8, and stored until later use. The samples were stored at 4 °C for 15-20 days before processing-a critical cold enrichment step-to enhance the recovery of *Y. pestis* and its bacteriophages. This prolonged incubation at a low temperature served a dual purpose: (1) it selectively inhibits the growth of fast-growing saprophytic and contaminating bacteria that could outcompete *Y. pestis* under standard culture conditions, and (2) it allows for the potential reactivation and amplification of slow-growing or stressed *Y. pestis* cells that might be present in the sample, thereby increasing the likelihood of phage detection. This method was adapted from established protocols for the isolation of slow-growing and fastidious pathogens.[14,15]

Isolation and identification of plague bacteriophages

EV76 strains in the logarithmic growth phase (200 µL) and 10 mL of LB liquid medium were added to a 50 mL centrifuge tube containing the HQG8 filtrate. The tube was incubated at 28 °C for 18-24 hrs at 180 rpm and the liquid state (clear or turbid) was observed after incubation. Thereafter, the solution was filtered through 0.22 µm filter membrane and stored at 4 °C. EV76 filtrate (200 µL and 100 µL) were added to a 1.5 mL centrifuge tube for 10 min, then LB semi-solid medium was added at approximately 45 °C, and poured onto a prepared LB plate to mix uniformly. The plate was then incubated at 28 °C for 18-24 hrs to observe the presence of phage plaques. For the negative control, 200 µL of LB liquid medium (without the host bacteria EV76) was added to the LB semi-solid medium (prepared as above) and poured onto a clean LB plate, and

then incubated at 28 °C for 18-24 hrs. For the parallel controls, the same volume of the filtrate from non-infected (with phage) EV76 cultures (or other appropriate non-target samples) was added to the LB semi-solid medium following the same procedure as the positive group, and also incubated at 28 °C for 18-24 hrs. These controls were established simultaneously with the positive group. The results can only be determined if a negative control is established, and the presence of phage plaques indicates the presence of a host bacterial phage.

Host range determination and the lysis property of bacteriophages

The lytic activity of HQG8 against various bacterial strains was determined using the spot assay. Briefly, fresh overnight cultures of indicator strains (including EV76) were mixed with soft agar and overlaid onto LB agar plates. After solidification, a 10 µL droplet of high-titer HQG8 lysate (≥10^8 Plaque Forming Units (PFU)/mL) was spotted onto the bacterial lawn. Notably, the bacterial growth phase and agar medium composition for this spot assay differed slightly from the optimal conditions used for plaque formation with EV76 during phage propagation. Plates were incubated at 22, 28, and 37 °C and examined for clearance zones after 18-24 hrs.

Plates were examined for the presence of a clearance zone (plaque) in a specific spot. The results were scored as follows: a clear or semi-clear zone (+) indicated susceptibility (lysis), whereas confluent bacterial growth identical to that of the surrounding lawn (-) indicated resistance (no lysis). Notably, the bacterial physiological state and agar medium composition for this spot assay were optimized for broad screening and differed slightly from the conditions used for efficient plaque formation with the propagation host EV76. To ensure the reliability and reproducibility of the results, each host range assay was performed with three independent biological replicates. Each replicate was initiated from a separate colony of each indicator strain. Furthermore, the entire spot test for each bacterium–phage combination was conducted in technical duplicate on separate plates for each biological replicate.

The general biological characteristics of plague bacteriophages

Determination of the optimal multiplicity of infection (MOI)

The adjusted ratio and addition amount were calculated based on the determined phage titer and the concentration of the host bacterial culture. Test tubes were labeled according to the following target MOI values: 0.001, 0.01, 0.1, 1, 10, and 100. Bacteriophages and EV76 were added, and the LB culture medium was replenished until the total volume of each tube was the same. Three tubes were prepared for each gradient, with three replicates in each tube. The EV76 host tubes and pure phage tubes were used as controls and incubated at 28 °C in a shaker for 4-8 hrs at 150 rpm. Thereafter, 600 µL was centrifuged at 10,000 rpm for 1 min, and the supernatant was collected for continuous gradient dilution; subsequently, the bacteriophage titer was determined and the average value of two duplicate tubes was recorded. The EV76 host tubes and pure phage tubes were used as controls. After being incubated overnight in a constant temperature box at 28 °C, the growth status of the phage plaques were observed under light. The plates with the densest phage plaque growth were counted. The MOI value that yielded the plate with the highest phage plaque count was considered the optimal MOI. We confirmed that the EV76 and pure phage tubes were not contaminated.

One-step growth curve determination

Phage and host preparation

A high-titer stock of HQG8 (≥10^8 PFU/mL) and a fresh overnight culture of the host bacterium *Y. pestis* EV76 were prepared. The EV76 culture was diluted 1:100 in fresh LB broth and incubated at 28 °C with shaking (180 rpm) until the mid-logarithmic phase (optical density at 600 nm [OD_{600}] ≈ 0.5). The concentration of viable bacteria was determined by plating serial dilutions on LB agar and counting the number of colony-forming units per milliliter (CFU/mL).

Infection and adsorption

The phages and bacteria were mixed at a predetermined MOI of 0.1 to a final volume of 1 mL. The mixture was incubated at 28 °C for 15 min to allow for phage adsorption.

Removal of unadsorbed phage

After the adsorption period, the mixture was centrifuged at 8,000 × *g* for 1 min in a microcentrifuge to create a pellet of bacteria and cell-associated phages. The supernatant, containing the unadsorbed free phages, was carefully removed and discarded. The pellet was resuspended in 1 mL of pre-warmed (28 °C) LB broth to remove residual unadsorbed phages and centrifuged again under the same conditions (8,000 × *g* for 1 min). This washing step was repeated. After a final wash, the supernatant was discarded completely.

Dilution and Incubation

The resulting pellet, containing infected cells, was immediately resuspended in 10 mL of pre-warmed (28 °C) LB broth to dilute the sample, thereby preventing secondary infection cycles. This moment was defined as time zero (t = 0). The culture was then incubated at 28 °C with shaking at 150 rpm.

Sampling and plaque assay

Beginning immediately at t = 0, 100 µL aliquots were collected from the culture at 20 min intervals for 180 min. Each sample was immediately centrifuged at 12,000 × *g* for 2 min to form cell pellets. The supernatant containing the progeny phages released from the lysed cells was carefully collected. The supernatant was serially diluted (10-fold) in LB broth, and the phage titer (plaque-forming units [PFU]/mL) at each time point was determined using a standard double-layer agar plaque assay as previously described. Each titration was performed in duplicate.

Data analysis

The phage titer (log10 PFU/mL) was plotted against the time post-dilution (minutes). The resulting one-step growth curve was used to determine the latent period (time from dilution until the first increase in titer), the rise period (time during which progeny phages were released), and the burst size (number of phages released per infected cell), calculated as the ratio of the final phage titer plateau to the initial titer of infected cells.

Observation of the optimal lysis temperature

Single EV76 colonies were obtained by drawing three streaks on solid medium, then incubating them in a constant temperature box at 22, 28, and 37 °C for cultivation and observation.

Genomic DNA Extraction, Sequencing, and Bioinformatic Analysis of Bacteriophage HQG8

Phage propagation and DNA extraction

Propagation of the bacteriophage HQG8 was initiated by infecting the host bacterium, *Y. pestis* EV76 strain, during the mid-logarithmic growth phase. The host-phage co-culture was incubated in LB broth at 28 °C with shaking (220 rpm) for 24 hrs. The resulting lysate was clarified by centrifugation and filtration through a 0.22 µm pore-size membrane to remove bacterial debris. Phage particles were subsequently concentrated by precipitation with polyethylene glycol (PEG) 8000 precipitation. Briefly, the clarified lysate was treated with DNase I and RNase A (1 µg/mL each) to degrade free nucleic acids, followed by the addition of EDTA (20 mM, pH 8.0) to chelate Mg^{2+} and halt nuclease activity. Phages were precipitated overnight at 4 °C using PEG 8000 (10% w/v) in the presence of 1 M NaCl. The pellet containing the concentrated phage particles was recovered by centrifugation and served as the starting material for genomic DNA extraction, which was performed using a commercial viral DNA kit (Beijing Aibigen Biotechnology Co. Ltd., Beijing, China) according to the manufacturer's instructions. The integrity and quality of the extracted DNA were verified by 1% agarose gel electrophoresis prior to downstream applications.

Whole-genome sequencing and assembly

High-quality genomic DNA was submitted to Novogene Co. Ltd., (Beijing, China) for whole-genome sequencing using an Illumina platform to generate paired-end reads (2 × 150 bp). The raw sequencing reads were subjected to quality control and adapter trimming. De novo genome assembly was performed using SPAdes (version 3.15.5) with default parameters, yielding a single, complete genomic contig for the bacteriophage HQG8.

Bioinformatics analysis and genome annotation

The assembled HQG8 genome was comprehensively characterized using a suite of bioinformatic tools. Fundamental genomic features, including size, GC content, and nucleotide composition, were calculated using the EditSeq module of the DNAStar software package. Tandem repetitive sequences were identified using Tandem Repeats Finder (TRF). Protein-coding sequences (CDSs) were predicted using a combination of Glimmer (version 3.0) and GeneMarkS, and the resulting open reading frames (ORFs) were functionally annotated by performing BLASTP searches (E-value cutoff $<1e^{-5}$) against the NCBI non-redundant (NR), Clusters of Orthologous Groups (COG), Gene Ontology (GO), and Kyoto Encyclopedia of Genes and Genomes (KEGG) databases. Transfer RNAs (tRNAs) were predicted using the tRNAscan-SE.

Comparative genomic and phylogenetic analysis

A comparative genomics approach was employed to elucidate the evolutionary relationship of HQG8. The genome was compared to those of related bacteriophages available in public databases using BLASTN. Average Nucleotide Identity (ANI) values were calculated to quantify genomic similarity. For a more granular analysis, specific genes of interest, such as those encoding structural proteins (e.g. major capsid and tail fiber proteins), were used as queries for targeted homology searches using SmartBLAST. Phylogenetic analyses were conducted based on the alignment of conserved protein sequences or whole-genome sequences. Multiple sequence alignments were generated using MUSCLE, and maximum-likelihood phylogenetic trees were constructed using the MEGA software (version 11), employing 1000 bootstrap replicates to assess node support.

RESULTS AND DISCUSSION

Isolation and identification of Plague bacteriophages

The optimal lysis temperature of the *Y. pestis* phage host bacterium EV76 isolated from dogs in wild rat plague foci was determined. When cultured within the range of 22-37 °C for 24 hrs, the growth condition of EV76 control was good and pollutant-free. The influence of the incubation temperature on plaque formation was assessed quantitatively. Plaque assays were performed in triplicate at 22, 28, and 37 °C using the double-layer agar method with EV76 as the host bacterium. After 24 hrs of incubation, plaque morphology and counts were analyzed. At 22 °C, plaque formation was inefficient, producing fewer than 10 plaques per plate with a small diameter of 0.3 ± 0.1 mm, and the plaques appeared turbid. In contrast, incubation at 28 °C yielded the highest plating efficiency, with an average of 152 ± 21 clear, distinct plaques per plate and a significantly larger ($p < 0.01$) mean diameter of 1.2 ± 0.2 mm (Figure 1). The efficiency of plating (EOP), calculated as the ratio of the plaque count at the test temperature to that at the optimal temperature (28 °C), was approximately 0.06 at 22 °C. At 37 °C, while the plaque count remained high (145 ± 18 PFU/plate), the plaques were notably larger but often exhibited a turbid halo, and some plates showed near-confluent lysis, indicating potentially altered phage-host dynamics at this temperature (EOP ≈ 0.95). These quantitative data demonstrate that 28 °C is the optimal temperature for efficient plaque formation by phage HQG8 on EV76, balancing high efficiency of infection with the production of clear, countable plaques. The observed plaque morphology (clear vs. turbid) served as a direct visual indicator of the infection efficiency. The small, turbid plaques at 22 °C correlate with poor adsorption or replication, whereas the large, turbid halos at 37 °C, despite a high EOP, suggest inefficient or asynchronous lysis, potentially reducing the effective burst size.

This study revealed the key influence of temperature on the efficiency of *Y. pestis* phages in lysing EV76 host bacteria. Experiments show that the formation of phage plaques optimizes with increasing temperature, reaching the optimal state at 28 °C, presenting as circular transparent plaques with a diameter of approximately 1 mm. This temperature may simultaneously align with the peak metabolic activity of the host bacterium EV76 and the efficient operation of the phage enzyme system, promoting the integrity of the adsorption-replication-lysis cycle and thereby enhancing the lysis efficiency.

High temperatures can alter the expression or structure of bacterial surface

receptors, reducing their accessibility or affinity for phage binding.[16,17] For example, in *Listeria monocytogenes*, less accessible rhamnose (a phage receptor) at 37 °C led to significantly reduced adsorption efficiency for certain phages.[18] Not all viruses or the cells they infect respond in the same way. Some phages can still adhere to certain objects at higher temperatures, while others are strongly affected. For example, the *Staphylococcus aureus* phage phiIPLA-RODI showed reduced adsorption at 37 °C in some strains but not others, likely due to temperature-dependent changes in wall teichoic acid glycosylation.[19]

Plaque assays were performed using the double-layer agar method. Briefly, mid-logarithmic phase *Y. pestis* EV76 was mixed with soft agar (0.7% w/v) and overlaid on an LB agar plate. A 10-fold serial dilution of HQG8 lysate was spotted onto the bacterial lawn, and the plate was incubated at 28 °C for 24 hrs. The plaques appear as clear, circular zones with an average diameter of 1.2 ± 0.2 mm, indicating efficient lytic activity under these conditions.

Morphology of bacteriophages

The morphology of *Y. pestis* bacteriophages was observed under a transmission electron microscope (TEM) after negative staining with 1% uranium peroxide acetate. The representative *Y. pestis* bacteriophage HQG8 had a head diameter of 65 nm and a tail length of 142 nm. It takes the form of a typical tadpole, consisting of a head with a regular icosahedral structure, a middle ring-shaped neck ring, and a long retractable tail sheath, which conforms to the morphological classification criteria of the *Myoviridae* family (Figure 2).[20,21] The head structure is conducive to the packaging of genetic material, and the retractable tail may penetrate the host cell wall through mechanical force. The tail was significantly longer than that of similar bacteriophages, suggesting an adaptive evolution specific to the host of *Y. pestis*.[22,23]

Phage particles were purified using PEG precipitation, deposited onto carbon-coated grids, and negatively stained with 1% uranyl acetate. Imaging was performed using a transmission electron microscope (TEM) operating at 80 kV. The phage exhibited typical myovirus morphology, comprising an icosahedral head (approximately 65 nm in diameter, indicated by a white arrow) and a long, contractile tail sheath (approximately 142 nm in length, indicated by a black arrow). Scale bar = 100 nm.

One-step growth curve of bacteriophages

A one-step growth curve of phage HQG8 is shown in Figure 3. The latent period, defined as the time interval from the moment of dilution (t = 0 min) until the first significant increase in the phage titer was 40 min. Following the latent period, the phage titer increased rapidly during the rise period (or burst period), which lasted for approximately 100 min, until it reached a plateau at approximately 140 min. The burst size average number of viable phage particles released per infected cell was calculated directly from the

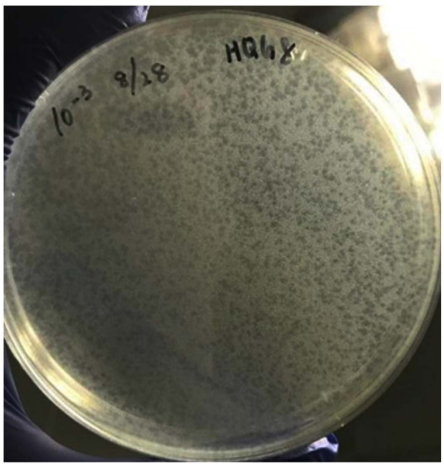

Figure 1. Plaque morphology of bacteriophage HQG8 on *Yersinia pestis* EV76

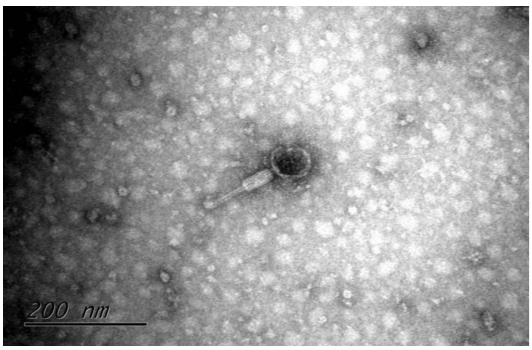

Figure 2. Transmission electron micrograph of bacteriophage HQG8

growth curve. It was determined as the ratio of the final phage titer plateau (approximately 1.5 × 10^8 PFU/mL) to the initial titer of infected cells at the beginning of the latent period (approximately 1.5 × 10^6 PFU/mL). The burst size was calculated to be approximately 100 PFU/infected cell (1.5 × 10^8 / 1.5 × 10^6 = 100). This high reproductive yield is functionally consistent with the efficient structural morphology of HQG8 observed under TEM (Figure 2); the icosahedral head is optimized for packaging genetic material, and the long contractile tail is likely to be highly effective in penetrating the host cell wall, working together to enable the efficient lytic cycle reflected in the growth curve.

This study revealed the dynamic characteristics of the lysis cycle of the plague phage HQG8 using a one-step growth curve. Calculation of the results of lysis amount showed that a single host bacterium could release numerous progeny bacteriophages, suggesting that HQG8 has efficient genomic replication and assembly capabilities. This may be closely related to the morphological characteristics observed using TEM, such as the icosahedral head structure and long contracting tail.[24,25] After 180 min, the bacteriophage titer tended to stabilize, indicating that the host bacterial population was fully lysed and the system reached a dynamic equilibrium. Notably, a longer lysis cycle (140 min) may reflect the adaptability of HQG8 to a specific infection strategy of *Y. pestis*, such as prolonging the DNA replication time to optimize the maturity of the offspring.[26]

Yersinia pestis EV76 cultures in the mid-logarithmic phase were infected with HQG8 at an MOI of 0.1. After a 15 min adsorption period at 28 °C, unadsorbed phages were removed by centrifugation and washing. Infected cells were resuspended in fresh pre-warmed LB broth and incubated at 28 °C with shaking. Samples were collected at the indicated time points, centrifuged immediately, and the supernatant was titrated using a plaque assay to determine the number of released phage particles (PFU/mL). The latent period (<H40 min), rise period (<H100 min), and burst size (approximately 100 PFU/infected cell) are indicated. Data points represent the mean ± standard deviation from three independent experiments.

The lysis property of bacteriophages

The HQG8 pairs of 20 *Y. pestis* strains isolated from dogs in wild rat plague foci of Heqing County almost all showed no lysis at 22 °C but showed lysis at 28 °C and 37 °C . HQG8 exhibited lysis characteristics against *Shigella flexneri* 2a at 22, 28, and 37 °C, and also exhibited lysis characteristics against *Shigella flexneri* X variant at 28 °C and 37 °C (Table and Figure 4).

It showed that the broad-spectrum cleavage of functional *Shigella flexneri* 2a by HQG8 (22-37 °C) sharply contrasts its selective

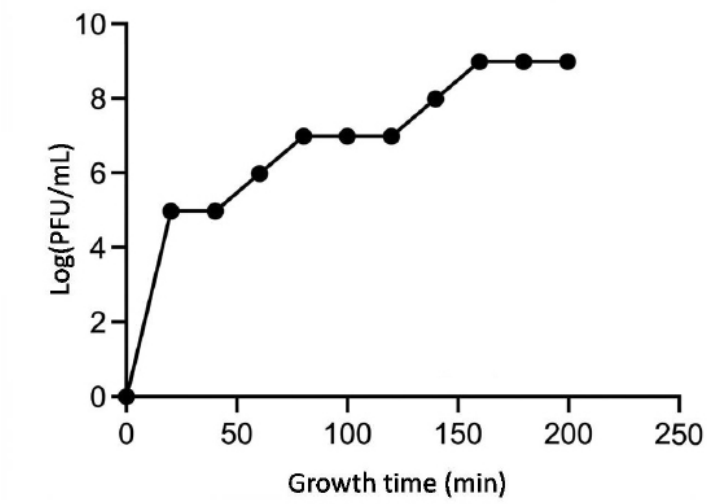

Figure 3. One-step growth curve of HQG8 plague bacteriophage

cleavage of *Shigella flexneri* X (only 28-37 °C), suggesting that its tail filament protein may recognize different host recipient epitopes through temperature-dependent conformational changes. Combined with the previous TEM observation results (tail contraction state), it is speculated that 28 °C may achieve efficient lysis in *Y. pestis* and *Shigella flexneri* X by regulating the contraction kinetics of tail sheath, optimizing host recognition and DNA injection efficiency. Structural studies reveal that mutations in the tail spike protein can expand or shift the phage host range by altering binding affinity for different O-antigen variants or by increasing reliance on secondary protein receptors.[27,28] Some phages possess multiple tail fibers or hybrid tail structures, enabling recognition of diverse host epitopes and adaptation to new hosts.[29] Temperature can influence the conformation of both the phage tail filament protein and bacterial surface structures, affecting binding and infection.[30] Some phages exhibit temperature-dependent infection cycles, switching between lytic and lysogenic states based on environmental temperature, which may be linked to conformational changes in tail proteins and receptor accessibility.[31] This study provides a new perspective for explaining the cleavage mechanism of temperature host dual regulation.

A critical and seemingly paradoxical observation was that the EV76 strain, which served as a propagation host for HQG8 isolation and plaque formation, was not lysed by the phage in the standardized spot assay (Table). This apparent contradiction can be explained by the profound influence of the bacterial physiological state and assay methodology on phage host interactions. During the initial phage isolation and plaque assay, EV76 was in a vigorous logarithmic growth phase on fresh agar medium, a condition during which the expression and conformation of bacterial surface receptors is optimized, thereby facilitating efficient phage adsorption and infection.[32] The clear plaques observed (Figure 1) unequivocally demonstrate that EV76 is a permissive host for HQG8 replication under these specific conditions. In contrast, the spot assay used for host range determination, which is highly valuable for broad screening, employs bacterial lawns that may represent different physiological states (e.g., cell density, growth phase, or receptor accessibility).[33] It is well documented that even minor variations in assay conditions can result in significant differences in observed bacteriophage lytic activity.[34,35] Furthermore, our study highlights the context-dependent nature of phage lytic activity. The inability of HQG8 to lyse its propagation host (EV76) in the spot assay despite efficient plaque formation (Figure 1), suggests that susceptibility assays can yield different outcomes based on the methodological parameters. This highlights the importance of defining the 'permissive host' (capable of supporting phage replication) separately from the 'susceptible host' (showing clear lysis in a spot or liquid assay) in phage characterization studies.[36]

Table. Host range of bacteriophage HQG8 against various bacterial strains

Test strain	HQG8 22 °C	HQG8 28 °C	HQG8 37 °C
Yersinia pestis 428	-	+	-
Yersinia pestis 488	-	+	-
Yersinia pestis 1318	-	+	+
Yersinia pestis 1396	-	+	+
Yersinia pestis 1412	-	+	-
Yersinia pestis 1413	-	+	-
Yersinia pestis 1672	-	+	+
Yersinia pestis 1751	-	+	-
Yersinia pestis YL236	-	+	+
Yersinia pestis YL261	-	+	+
Yersinia pestis 1755	-	+	+
Yersinia pestis 1814	-	+	-
Yersinia pestis 2036	-	+	+
Yersinia pestis 2037	-	+	+
Yersinia pestis 2083	-	+	+
Yersinia pestis 2131	-	+	+
Yersinia pestis 2237	-	+	+
Yersinia pestis YL179	-	+	+
Yersinia pestis YL258	-	+	+
Yersinia pestis HQ153	-	+	+
EV76	-	-	-
Shigella flexneri 2a	+	+	+
Shigella flexneri X variant	-	+	+
Pseudomonas aeruginosa type 47	-	-	-

Note: Lysis activity was determined by a spot test assay. +, clear or semi-clear zone of inhibition (positive for lysis); -, confluent bacterial growth without a zone (negative for lysis). EV76 served as the propagation host for phage isolation

The biological and evolutionary implications of HQG8's lytic activity against *Shigella*

The observed lytic activity of HQG8 against *Shigella flexneri*, particularly the broad-spectrum lysis of serotype 2a across all tested temperatures (22-37 °C), is a finding of significant biological relevance. This cross-genus activity suggests that HQG8 may recognizes a highly conserved surface receptor common to both *Y. pestis* and certain *Shigella* species. The receptor may be a core component of the lipopolysaccharide (LPS) O-antigen or an outer membrane protein. This hypothesis is strongly supported by structural studies of *Shigella* phages, which have identified the tail spike protein as the key determinant for binding to specific LPS O-antigen variants.[37] The

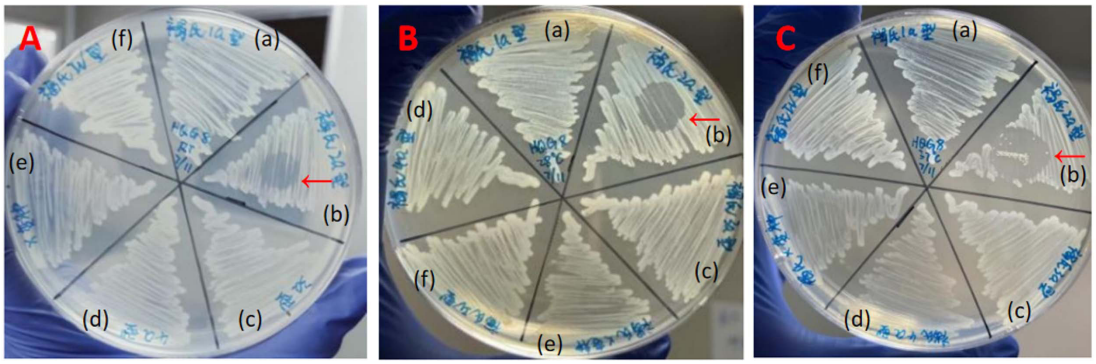

Figure 4. Host range determination of bacteriophage HQG8 against *Shigella* species at different temperatures. (A) at 22 °C; (B) at 28 °C; (C) at 37 °C. Lytic activity of bacteriophage HQG8 against various *Shigella* species at different temperatures. The plate was divided into six sectors inoculated with: (a) *S. flexneri* 1a, (b) *S. flexneri* 2a, (c) *S. flexneri* 3a, (d) *S. flexneri* 4a, (e) *S. flexneri* variant X, and (f) *S. flexneri* IV. Representative colonies were indicated by arrows. The plate was held using a gloved hand to maintain aseptic conditions

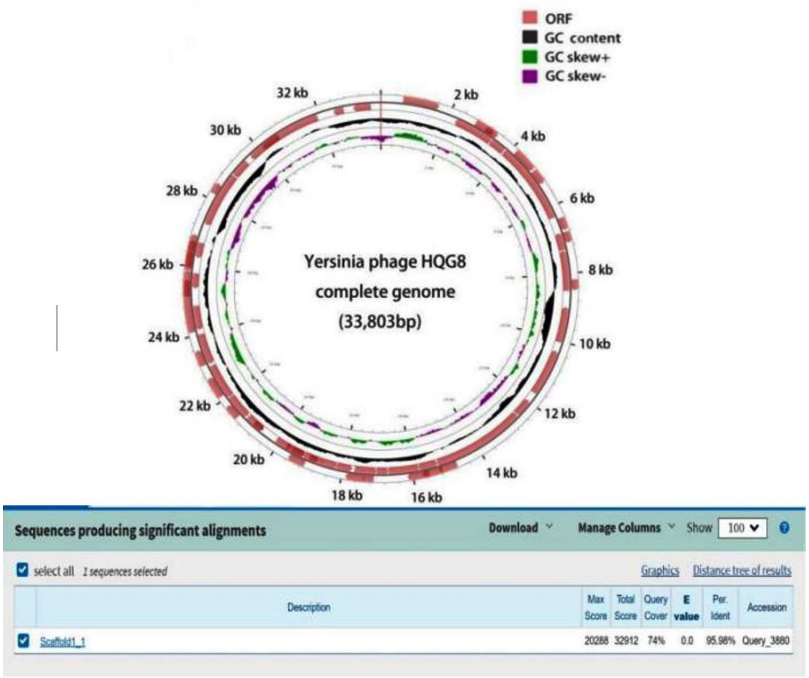

Figure 5. The full genome composition circle diagram of HQG8

temperature-dependent variation in lysis efficiency (e.g., for *Shigella flexneri* X variant) further suggests that the conformation or accessibility of this shared receptor is influenced by thermal conditions, affecting the initial adsorption step of the phage, a regulatory effect on phage adsorption that has been documented in other systems.[38] From an evolutionary perspective, the ability to infect enteric bacteria such as *Shigella* and *E. coli* (as suggested by high genomic homology) indicates that HQG8 likely originates from a common agar enterobacteriophage lineage. Its isolation from a dog during a plague may represent a recent host jump or an ongoing adaptation to *Y. pestis* within a unique ecological niche. This ecological plasticity underscores the dynamic nature of phage host ranges and highlights the potential of phages to traverse ecosystem boundaries, a phenomenon that has been explored in broader analyses of the prokaryotic virosphere.[39]

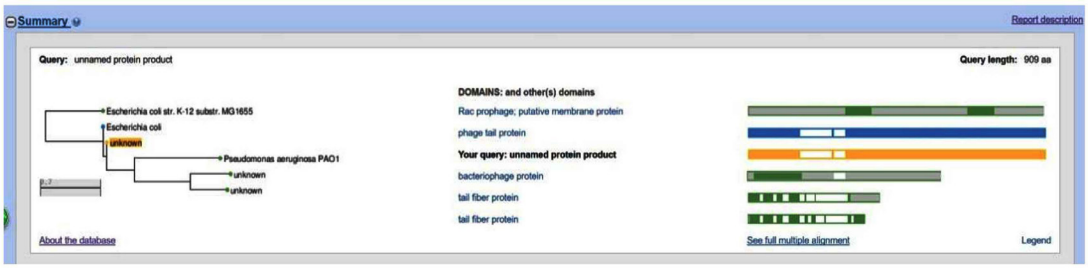

Figure 6. The ORF94 SmartBLAST comparison results of HQG8 (the yellow "unknown" in the query represents the open reading framework ORF94)

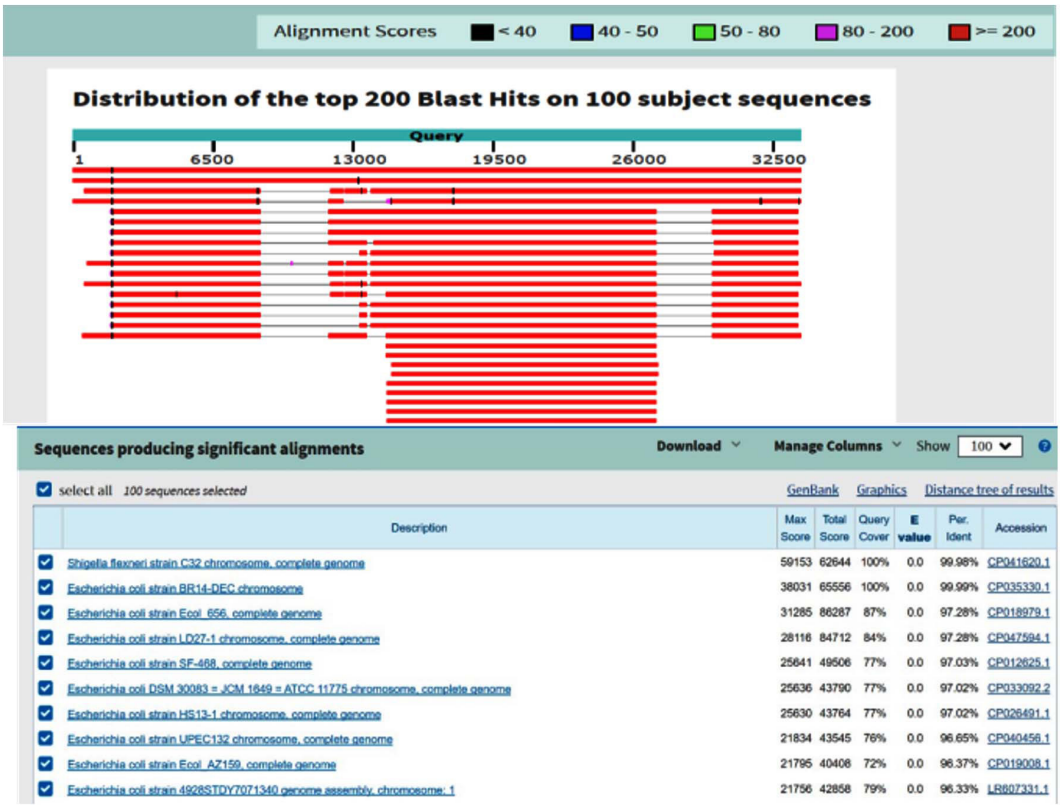

Figure 7. The comparison results between the HQG8 bacteriophage and the NCBI full gene bank

Genomic study of plague phage

Analysis of the general characteristics of the genome revealed that the total length of the gene sequence of HQG8 is 35,876 bp, with a GC content of 51.50%, accounting for 94.22% of the total genome length. Figure 5 shows the gene circle diagram of the complete gene sequence and composition of HQG8. The outer circle of the graph represents the gene-coding analysis, and the inner circle represents the CG bias analysis. The outward direction indicates a positive CG bias, whereas the inward direction indicates a negative CG bias. Through gene prediction, functional annotation, and protein comparison, it was discovered that HQG8 has 126 open reading frameworks, ranging from ORF1 to ORF126. One open reading framework (ORF94) was selected for SmartBLAST. ORF94 began at 15235 and ended at 12506, with a protein size of 909, as shown in Figure 6. A phylogenetic tree and graphical overview were created, and showed that this segment has a relatively high homology with *Pseudomonas aeruginosa* PAO1. This protein was mainly a hypothetical membrane protein; the tail filament protein of bacteriophages. Ten strains with high similarity were selected for homology analysis and compared to the whole genome in the NCBI library. The results showed that HQG8 shares 99.98% sequence homology across 100% gene coverage with *Shigella flexneri* C32 and 99.99% homology with the BR14-DEC gene of an *Escherichia coli* strain. The remaining isolates also exhibited high homology with the *Escherichia coli* strain. As shown in Figure 7, whole-genome homology analysis revealed that HQG8 shares more than 99.9% identity with enteric phages. This high degree of conservation suggests that HQG8 belongs to a widely distributed phage lineage. However, the identification of this phage lineage in a domestic dog from a plague-endemic focus is a significant finding. This indicates the potential for cross-species transmission and environmental persistence of these phages. Therefore, the functional novelty of HQG8 may lie not only in its genomic sequence, but also in its ecological niche and its ability to lyse *Y. pestis* under specific conditions, which merits further investigation.

The HQG8 phage, isolated from anal swab samples obtained from dogs within plague foci, was confirmed to be a plague bacteriophage with practical application potential. Further genomic research revealed significant phenomena in its evolution and functional adaptation. The HQG8 genome exhibits typical characteristics of a double-stranded DNA bacteriophage genome. Notably, genomic annotation revealed that the tail filament protein (ORF94) exhibited high sequence homology with the *P. aeruginosa* PAO1 bacteriophage. The tail filament protein was a key factor determining phage host specificity, responsible for recognizing specific receptors on bacterial surfaces.[40] However, in vitro host range assays revealed that HQG8 failed to lyse *P. aeruginosa* strain 47 at 22, 28, and 37 °C. This phenomenon indicated that despite sequence-level homology, its receptor-binding domain may have undergone functional variation, rendering it incapable of recognizing *P. aeruginosa*, reflecting the rapid evolution of phages to adapt to new hosts.[41] Furthermore, this phenomenon indicates that although conserved in sequence, its receptor-binding domain may have undergone functional differentiation through adaptive evolution, enabling it to specifically recognize the surface receptors of *Yersinia* or *Shigella*. Therefore, temperature may ultimately determine the infection efficiency and differences in plaque morphology by influencing the conformation of these differentiated tail silk proteins or by regulating the accessibility of host receptors. Whole-genome homology analysis revealed that the gene coverage of HQG8 with the *Shigella* bacteriophage C32 reached 100%, with 99.98% homology. It also exhibited a high degree of homology (99.99%) with the *Escherichia coli* bacteriophage BR14-DEC. This was consistent with the results of our previous lysis experiments and the background information obtained from the anal swabs. Notably, the lysis ability of HQG8 against *Y. pestis* EV76 is consistent with its specificity for Enterobacteriaceae hosts. Although the tail thread protein of this bacteriophage was evolutively homologous to that of the *Pseudomonas* bacteriophage, it has acquired the ability to recognize the surface receptors of *Yersinia* plague and *Shigella* through the exchange of gene modules and adaptive evolution.[39] This host-wide evolution revealed the molecular evolutionary mechanism of bacteriophages in adapting to different ecological environments. In addition, HQG8 maintained stable pyrolysis activity within

the range of 22-37 °C . This characteristic indicates that they can maintain good biological functions at different environmental temperatures, from the low-temperature external environments to the body temperature environment of mammals. This characteristic provided significant advantages for its application in the prevention and control of plague, especially in environmental monitoring and the handling of epidemic foci, where it had potential value.[42] In summary, the identification and functional study of the bacteriophage HQG8 demonstrated the significance of combining genomic analysis with experimental verification. The evolutionary history of its tail silk protein reflected the molecular innovation of bacteriophages to adapt to new hosts, and its specific cleavage ability against *Y. pestis* provides a solid foundation for application in biological control.

CONCLUSION

We successfully isolated and characterized HQG8, a bacteriophage with high genomic similarity to known enteric phages, and to our knowledge, this is the first report of its isolation from domestic dogs in a plague-endemic area. The novelty of this study lies in expanding the known ecological range of these phages and demonstrating their presence in an indicator animal species that is closely associated with human settlements. The temperature sensitivity of HQG8 underscores the environmental factors that influence phage-host interactions in natural reservoirs. Future studies should explore the ecological impact of phages on *Y. pestis* persistence, their applicability in phage-based diagnostics or therapeutics, and the molecular mechanisms underlying host specificity and temperature-regulated lytic behavior. These findings advance our understanding of plague microecology and provide a foundation for the development of novel strategies for plague surveillance and control.

ACKNOWLEDGMENTS

The authors would like to thank Yunnan Provincial Institute for the Prevention and Control of Endemic Diseases and its Central Laboratory for their assistance.

CONFLICT OF INTEREST

The authors declare that there is no conflict of interest.

AUTHORS' CONTRIBUTION

LY performed data collection. LY and XZ performed data analysis. SL performed investigation and data curation. LY wrote original draft. XZ supervised the study. BL wrote, reviewed, and edited the manuscript. All authors read and approved the final manuscript for publication.

FUNDING

This study was supported by Yunnan Provincial Department of Education through project numbers 2025J0775 and 2025Y1187.

DATA AVAILABILITY

All datasets generated or analyzed during this study are included in the manuscript.

ETHICS STATEMENT

This study was approved by the Yunnan Provincial Institute for the Prevention and Control of Endemic Diseases and its Central Laboratory

REFERENCES

1. Mishra V, Bankar N, Tiwade Y, Ugemuge S. How phage therapy works, its advantages and disadvantages: Mini review. *J Pure Appl Microbiol.* 2024;18(1):177-184. doi: 10.22207/JPAM.18.1.49
2. Nasr-Eldin MA, El-Dougdoug NK, Elazab YH, Esmael A. Isolation and characterization of two virulent phages to combat *Staphylococcus aureus* and *Enterococcus faecalis* causing dental caries. *J Pure Appl Microbiol.* 2021;15(1):320-334. doi: 10.22207/JPAM.15.1.25
3. Yuan Y, Xi H, Dai J, et al. The characteristics and genome analysis of the novel *Y. pestis* phage JC221. *Virus Res.* 2020;283:197982. doi: 10.1016/j.virusres.2020.197982
4. Zhong Y, Duan C, Guo Y, et al. Isolation and identification of plague phage from plague foci in Yulong County, Yunnan Province. *Chin J Endemiol*. 2018;37(12):707-710.
5. Jin H, Zhong Y, Wang Y, et al. Two novel yersinia pestis bacteriophages with a broad host range: Potential as biocontrol agents in plague natural foci. *Viruses.* 2022;14(12):2740. doi: 10.3390/v14122740
6. Kilgore PB, Sha J, Hendrix EK, et al. A bacteriophage cocktail targeting *Yersinia pestis* provides strong post-exposure protection in a rat pneumonic plague model. Denes TG, ed. *Microbiol Spectr.* 2024;12(11):e00942-24. doi: 10.1128/spectrum.00942-24

7. Wardani AK, Fitri RA, Ramadhani FR, Tarno H, Fibrianto K, Pertiwi FNE. Isolation and characterization of a phage xoo-Tp1, infecting *Xanthomonas oryzae* pv. *oryzae*. *J Pure Appl Microbiol.* 2025;19(3):1771-1781. doi: 10.22207/JPAM.19.3.50
8. Friderike B, Peter B, Holger C, et al. Specific detection of *Yersinia pestis* based on receptor binding proteins of phages. *Pathogens.* 2020;9(8):611. doi: 10.3390/pathogens9080611
9. Schofield DA, Molineux IJ, Westwater C. Diagnostic bioluminescent phage for detection of *Yersinia pestis*. *J Clin Microbiol.* 2009;47(12):3887-3894. doi: 10.1128/JCM.01533-09
10. Vagima Y, Gur D, Aftalion M, et al. Phage therapy potentiates second-line antibiotic treatment against pneumonic plague. *Viruses*. 2022;14:688. doi: 10.1101/2022.02.07.479346
11. Bonczarowska JH, Susat J, Krause-Kyora B, et al. Ancient *Y. pestis* genomes lack the virulence-associated Ypf Φ prophage present in modern pandemic strains. *Proc R Soc B.* 2023;290(2023):20230622. doi: 10.1098/rspb.2023.0622
12. Lyu D, Duan Q, Duan R, et al. Symbiosis of a lytic bacteriophage and *Yersinia pestis* and characteristics of plague in *Marmota himalayana*. *Appl Environ Microbiol.* 2024;90(8):e0099524. doi: 10.1128/aem.00995-24
13. Konyshev I, Dudina L, Belozerov V, et al. Biophysical and microbiological aspects of the interaction between *Yersinia pestis* PsaA and bacteriophage L-413C. *Eur Biophys J.* 2025;54(5):267-276. doi: 10.1007/s00249-025-01768-6
14. Pai CH, Sorger S, Lafleur L, Lackman L, Marks MI. Efficacy of cold enrichment techniques for recovery of *Yersinia enterocolitica* from human stools. *J Clin Microbiol.* 1979;9(6):712-715. doi: 10.1128/jcm.9.6.712-715.1979
15. Evaluation of isolation methods for pathogenic *Yersinia enterocolitica* from pig intestinal content. *J Appl Microbiol.* 2010;108(3):956-964. doi: 10.1111/j.1365-2672.2009.04494.x
16. Kering KK, Zhang X, Nyaruaba R, Yu J, Wei H. Application of adaptive evolution to improve the stability of bacteriophages during storage. *Viruses.* 2020;12(4):423. doi: 10.3390/v12040423
17. Chang RYK, Kwok PCL, Khanal D, et al. Inhalable bacteriophage powders: Glass transition temperature and bioactivity stabilization. *Bioeng Transl Med.* 2020;5(2):e10159. doi: 10.1002/btm2.10159
18. Tokman JI, Kent DJ, Wiedmann M, Denes T. Temperature significantly affects the plaquing and adsorption efficiencies of *Listeria* phages. *Front Microbiol.* 2016;7:631. doi: 10.3389/fmicb.2016.00631
19. Guo Y, Pfahler NM, Völpel SL, Stehle T. Cell wall glycosylation in *Staphylococcus aureus*: targeting the tar glycosyltransferases. *Curr Opin Struct Biol*. 2021;68:166-174. doi: 10.1016/j.sbi.2021.01.003
20. Novacek J, Siborova M, Benesik M, Pantucek R, Doskar J, Plevka P. Structure and genome release of twort-like myoviridae phage with a double-layered baseplate. *Proc Natl Acad Sci U S A.* 2016;113(33):9351-9356. doi: 10.1073/pnas.1605883113
21. Accetto T, Janež N. The lytic *Myoviridae* of *Enterobacteriaceae* form tight recombining assemblages separated by discontinuities in genome average nucleotide identity and lateral gene flow. *Microb Genom.* 2018;4(3). doi: 10.1099/mgen.0.000169
22. Shuzhen W, Anan W, Lanlan C, et al. Proteomic Analysis of Marine Bacteriophages: Structural Conservation, Post-Translational Modifications, and Phage–Host Interactions. *Environ Microbiol*. 2025;27(4):e70099. doi: 10.1111/1462-2920.70099
23. Skurnik M, Jaakkola S, Mattinen L, et al. Bacteriophages fEV-1 and fD1 infect *Yersinia pestis*. *Viruses.* 2021;13(7):1384. doi: 10.3390/v13071384
24. Wenyuan C, Hao X, Xurong W, et al. Structural changes of a bacteriophage upon DNA packaging and maturation. *Protein Cell.* 2020;11(5):374-379. doi: 10.1007/s13238-020-00715-9
25. Junrong L, Shuai Q, Ran D, et al. A lytic *Yersina pestis* bacteriophage obtained from the bone marrow of *Marmota himalayana* in a plague-focus area in China. *Front Cell Infect Microbiol.* 2021;11:322. doi: 10.3389/fcimb.2021.700322
26. Mabruka S, Maria IP, Jin W, at al. T4-like bacteriophages isolated from pig stools infect *Yersinia pseudotuberculosis* and *Yersinia pestis* using LPS and OmpF as receptors. *Viruses.* 2021;13(2):296. doi: 10.3390/v13020296
27. Sørensen AN, Woudstra C, Sørensen MCH. Brøndsted L. Subtypes of tail spike proteins predicts the host range of *Ackermannviridae* phages. *Comput Struct Biotechnol J*. 2021;19:4854-4867. doi: 10.1016/j.csbj.2021.08.030.
28. Subramanian S, Dover JA, Parent KN, Doore SM. Host range expansion of *Shigella phage* Sf6 evolves through point mutations in the tailspike. *J Virol.* 2022;96(16):14. doi: 10.1128/jvi.00929-22
29. Sundharraman S, Silje MBD, Kendal RT, Parent KN. Cryo-EM structure of a *Shigella podophage* reveals a hybrid tail and novel decoration proteins. *Structure.* 2024;32(1):24-34. doi: 10.1016/j.str.2023.10.007
30. Sonja K, Tom S, Saskia B, et al. Bacteriophage Sf6 tailspike protein for detection of *Shigella flexneri* pathogens. *Viruses*. 2018;10(8):431. doi: 10.3390/v10080431
31. Biao M, Zhizhen Q, Xiang L, et al. Characterization of mu-like *Yersinia* phages exhibiting temperature dependent infection. *Microbiol Spectr.* 2023;11(4):11. doi: 10.1128/spectrum.00203-23
32. Paul H, Stephen T. A. Bacteriophage host range and bacterial resistance. *Adv Appl Microbiol.* 2010;70:217-248. doi: 10.1016/S0065-2164(10)70007-1
33. Altamirano FLG, Barr JJ. Phage Therapy in the Postantibiotic Era. *Clin Microbiol Rev.* 2019;32(2):24. doi: 10.1128/cmr.00066-18
34. Mohammadali KM, Anders SN. Isolation of phages for phage therapy: A comparison of spot tests and efficiency of plating analyses for determination of host range and efficacy. *PLOS One.* 2015;10(5): e0127606. doi: 10.1371/journal.pone.0118557
35. Andrew MK. Practical Advice on the One-Step Growth Curve. In: Clokie M, Kropinski A, Lavigne R, ed.

Bacteriophages. Methods in Molecular Biology, vol 1681. Humana Press, New York, NY. doi: 10.1007/978-1-4939-7343-9_3

36. Dion MB, Oechslin F, Moineau S. Phage diversity, genomics and phylogeny. *Nat Rev Microbiol.* 2020;18(3):125-138. doi: 10.1038/s41579-019-0311-5
37. Subramanian S, Kerns HR, Braverman SG, Doore SM. The structure of *Shigella* virus Sf14 reveals the presence of two decoration proteins and two long tail fibers. *Commun Biol.* 2025;8(1):222. doi: 10.1038/s42003-025-07668-x
38. FernAndez L, Duarte AC, Jurado A, Bueres L, RodrIguez A, GarcIa P. Multipronged impact of environmental temperature on *Staphylococcus aureus* infection by phage kayvirus rodi: Implications for biofilm control. *Biofilm*. 2025;9:100248. doi: 10.1016/j.bioflm.2024.100248
39. Andre MC, Graham FH, Krisch HM, Lindell D, Mann NH, Prangishvili D. Exploring the prokaryotic virosphere. *Res Microbiol.* 2008;159(5):306-313. doi: 10.1016/j.resmic.2008.05.001
40. Nobrega FL, Vlot M, de Jonge PA, et al. Targeting mechanisms of tailed bacteriophages. *Nat Rev Microbiol.* 2018;16(12):760-773. doi: 10.1038/s41579-018-0070-8
41. Yehl K, Lemire S, Yang AC, et al. Engineering phage host-range and suppressing bacterial resistance through phage tail fiber mutagenesis. *Cell.* 2019;179(2):459-469. doi: 10.1016/j.cell.2019.09.015
42. Andrey AF, Kirill VS, Yunxiu H, et al. Bacteriophage Therapy of Experimental Bubonic Plague in Mice. In: de Almeida A, Leal N, ed. *Advances in Yersinia Research. Advances in Experimental Medicine and Biology*, vol 954. Springer, New York, NY. 2012;954(1):337-348. doi: 10.1007/978-1-4614-3561-7_41